Supporting Information

Supramolecular dual-donor artificial light-harvesting system with efficient visible light-harvesting capacity

Yi-Xiong Hu,[†] Pei-Pei Jia,[†] Chang-Wei Zhang, [†] Xing-Dong Xu,[,‡] Yanfei Niu,[†] Xiaoli Zhao,[†] Qian Xu, [‡] Lin Xu*[,†] and Hai-Bo Yang*[,†]*

[†]Shanghai Key Laboratory of Green Chemistry and Chemical Processes, School of Chemistry and Molecular Engineering, East China Normal University, 3663 N. Zhongshan Road, Shanghai 200062, P. R. China

[‡]Key Laboratory of Special Functional Aggregated Materials of Ministry of Education, School of Chemistry and Chemical Engineering, National Engineering Research Center for Colloidal Materials, Shandong University, Jinan, Shandong 250100, P. R. China

Email address: xuxd@sdu.edu.cn (X.-D. X.), lxu@chem.ecnu.edu.cn (L. X.), hbyang@chem.ecnu.edu.cn (H.-B. Y.)

Table of Contents

Section A. Materials and general methods

All reagents and compounds **6**, **S2** and **S3** were commercially available and used as supplied without further purification, compounds **1**, **2**, and **S1** were prepared according to the published procedures[S1-S3].

All solvents were dried according to standard procedures and all of them were degassed under N_2 for 30 minutes before use. All air-sensitive reactions were carried out under inert N_2 atmosphere. ^{1}H NMR, ^{13}C NMR and ^{31}P NMR spectra were recorded on Bruker 400 MHz Spectrometer (^{1}H: 400 MHz; ^{13}C: 101 MHz, ^{31}P: 162 MHz) and Bruker 500 MHz Spectrometer (^{1}H: 500 MHz; ^{13}C: 126 MHz, ^{31}P: 202 MHz) at 298 K. The ^{1}H and ^{13}C NMR chemical shifts are reported relative to residual solvent signals, and ^{31}P {^{1}H} NMR chemical shifts are referenced to an external unlocked sample of 85% H_3PO_4 (δ 0.0). 2D NMR spectra (^{1}H-^{1}H COSY, NOESY and DOSY) were recorded on Bruker 500 MHz Spectrometer (^{1}H: 500 MHz) at 298 K. The MALDI MS experiments were carried out on a Bruker UltrafleXtreme MALDI TOF/TOF Mass Spectrometer (Bruker Daltonics, Billerica, MA), equipped with smartbeam-II laser. All spectra were measured in positive reflectron or linear mode. UV-vis spectra were recorded in a quartz cell (light path 10 mm) on a Cary 50Bio UV-visible spectrophotometer. Fluorescence spectra were recorded in a conventional quartz cell (light path 2 mm) on a Cary Eclipse fluorescence spectrophotometer. Fluorescence quantum yields were measured in absolutely in solution using a commercial fluorometer with integrating sphere (RF6000, shimadzu). Fluorescence lifetimes were measured based on TCSPC technique. The squared deviations obtained by the least-squares analysis was utilized to estimate the fitting of TCSPC data and judge the multiexponential emission decay processes.

Section B. Synthesis and characterization of new compounds.

1. Synthesis and characterization of metallacycle 3.

Scheme S1: Self-assembly of supramolecular [2 + 2] metallacycle **3** from dipyridyl donor ligand **1** and diplatinum acceptor **2**.

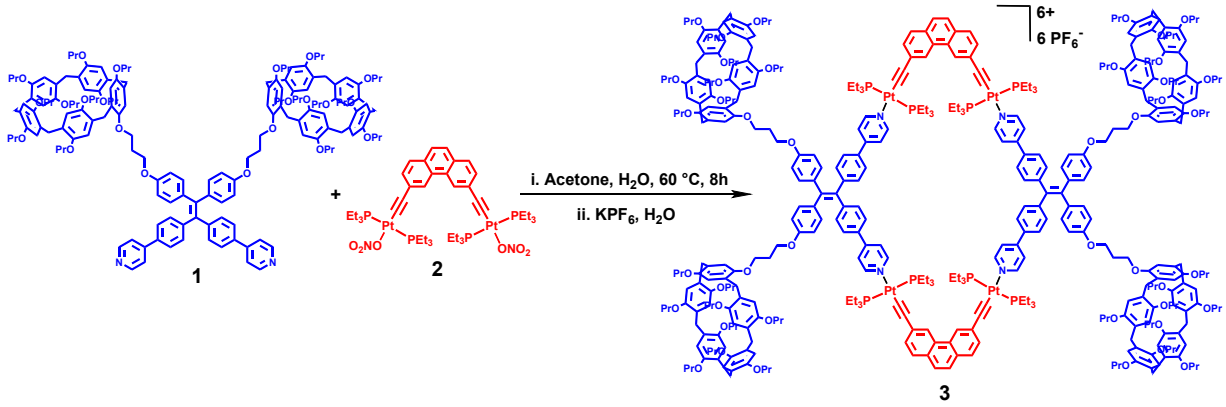

Synthesis of 3: The dipyridyl donor ligand **1** (25.4 mg, 9.86 μmol) and the 60° diplatinum acceptor **2** (12.0 mg, 9.86 μmol) were weighed accurately into a glass vial. To the vial was added 2.0 mL of acetone and 0.4 mL of water, and the reaction solution was then stirred at 60 °C for 8 h to yield a homogeneous yellow solution. Then the addition of a saturated aqueous solution of KPF_6 into the bottle with continuous stirring (10 min) precipitated the product. The reaction mixture was centrifuged, washed several times with water, and dried. Yellow solid product **3** was obtained by removing the solvent under vacuum. Yield: 35.9 mg, 92%. ^{1}H NMR (500 MHz, acetone-d_6): δ 8.97-8.96 (d, J = 5.0 Hz, 8H), 8.57 (s, 4H), 8.11-8.10 (d, J = 5.0 Hz, 8H), 7.93-7.91 (d, J = 10.0 Hz, 4H), 7.85-7.84 (d, J = 5.0 Hz, 8H), 7.78 (s, 4H), 7.60-7.59 (d, J = 5.0 Hz, 4H), 7.34-7.33 (d, J = 5.0 Hz, 8H), 7.11-7.09 (d, J = 5.0 Hz, 8H), 6.93-6.88 (m, 48H), 4.30-4.27 (t, J = 7.5 Hz, 8H), 4.08-4.05 (t, J = 7.5 Hz, 8H), 3.84-3.76 (m, 72H), 2.34-2.32 (t, J = 5.0 Hz, 8H), 2.04-2.03 (m, 48H), 1.89-1.75 (m, 72H), 1.33-1.26 (m, 72H), 1.12-1.00 (m, 108H). ^{13}C NMR (126 MHz, acetone-d_6): δ 8.97, 8.96, 8.57, 8.11, 8.10, 7.93, 7.91, 7.85, 7.84, 7.78, 7.60, 7.59, 7.34, 7.33, 7.11, 7.09, 6.93, 6.91, 6.90, 6.89, 6.88, 4.30, 4.28, 4.27, 4.08, 4.06, 4.05, 3.84, 3.83, 3.82, 3.81, 3.80, 3.78, 3.76, 3.76, 3.76, 2.34, 2.33, 2.32, 2.04, 2.04, 2.03, 1.89, 1.88, 1.86, 1.85, 1.84, 1.82, 1.81, 1.79, 1.78, 1.76, 1.75, 1.33, 1.31, 1.29, 1.28, 1.26, 1.12, 1.11, 1.09, 1.09, 1.08, 1.07, 1.06, 1.04, 1.03, 1.02, 1.00. ^{31}P NMR (202 MHz, acetone-d_6): δ 15.72 ($^1J_{Pt\text{-}P}$ = 2335.12 Hz). MS (ESI-MS): *m/z* calcd for $[M - 4PF_6]^{4+}$: 1832.1687, found: 1832.1034; *m/z* calcd for $[M - 3PF_6]^{3+}$: 2491.2131, found: 2491.1258.

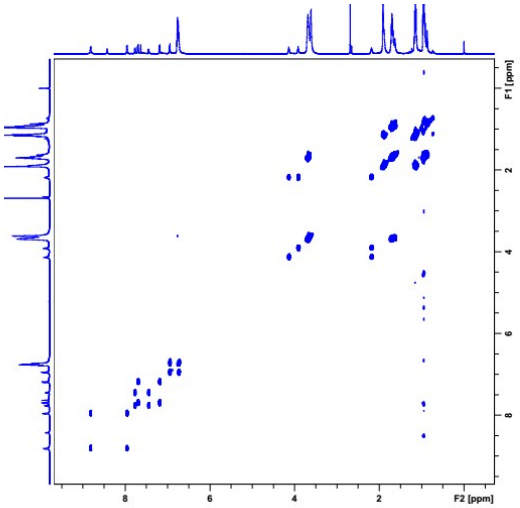

Fig. S1. 2D COSY NMR (500 MHz, acetone-d_6, 298 K) spectrum of metallacycle **3**.

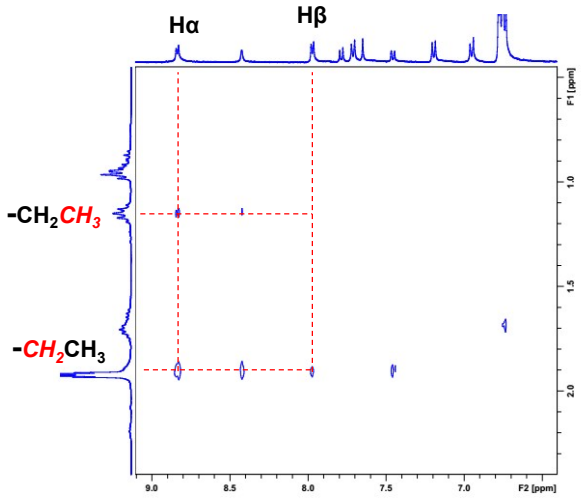

Fig. S2. Partial 2D NOESY NMR (500 MHz, acetone-d_6, 298 K) spectrum of metallacycle **3**. (The signals in spectra indicated the formation of Pt-N bonds).

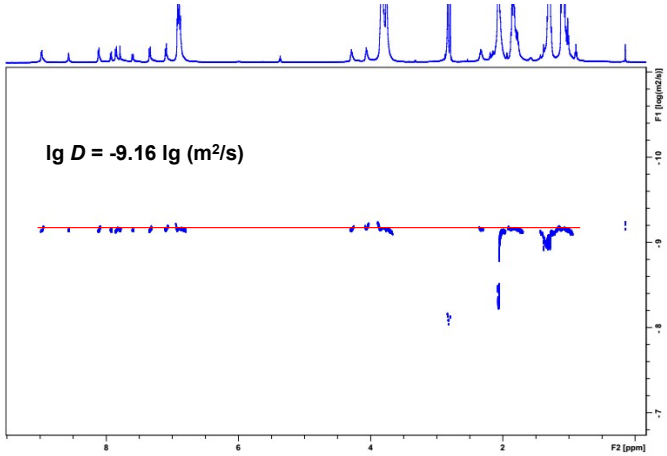

Fig. S3. 2D DOSY NMR (500 MHz, acetone-d_6, 298 K) spectrum of metallacycle **3**.

2. Synthesis and characterization of compounds 4 and 5.

Scheme S2: The synthesis route of compound **4**.

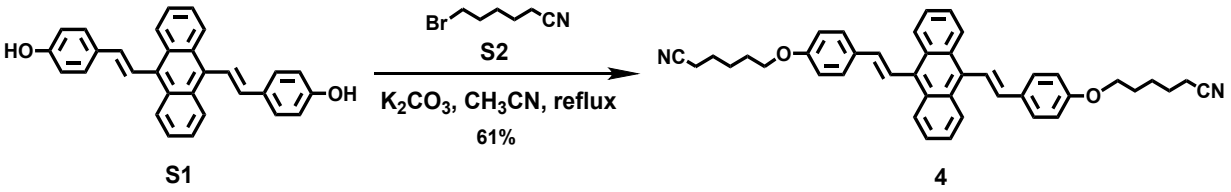

Synthesis of 4: A solution of compound **S1** (0.33 g, 0.80 mmol) and K_2CO_3 (0.44 g, 3.2 mmol) in dry CH_3CN (40 mL) was heated at reflux for 5 min under nitrogen atmosphere, and then a solution of compound **S2** (0.56 g, 3.2 mmol) in dry CH_3CN (15 mL) was added. The solution was heated at reflux for 22 hours. After the solid was filtered, the solvent was removed by evaporation on a rotary evaporator. The residue was purified by column chromatography on silica gel to give compound **4** as a white solid (294 mg, 61%). ^{1}H NMR (400 MHz, $CDCl_3$): δ 8.41-8.39 (m, 4H), 7.81-7.77 (d, J = 10.0 Hz, 2H), 7.63-7.61 (d, J = 5.0 Hz, 4H), 7.47-7.45 (m, 4H), 6.99-6.97 (d, J = 5.0 Hz, 4H), 6.89-6.86 (d, J = 7.5 Hz, 2H), 4.07-4.05 (t, J = 5.0 Hz, 4H), 2.43-2.41 (t, J = 5.0 Hz, 4H), 1.91-1.86 (m, 4H), 1.82-1.76 (m, 4H), 1.73-1.68 (m, 4H). ^{13}C NMR (126 MHz, $CDCl_3$): δ 159.03, 136.97, 132.92, 130.43, 129.78, 127.98, 126.67, 125.26, 123.10, 119.76, 114.94, 67.64, 28.65, 25.60, 25.38, 17.35. MS (MALDI-TOF): Calculated for [**4**]$^+$: 604.3; Found: 604.2.

Scheme S3: The synthesis route of compound **5**.

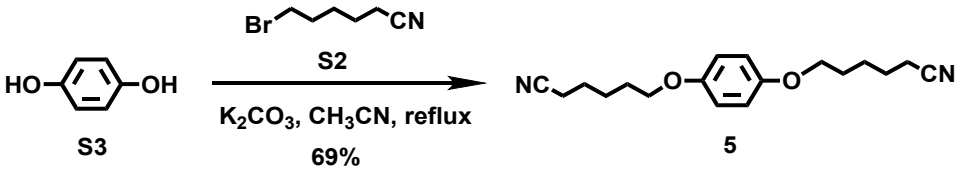

Synthesis of 5: A solution of Hydroquinone **S3** (0.30 g, 2.72 mmol) and K_2CO_3 (1.50 g, 10.88 mmol) in dry CH_3CN (25 mL) was heated at reflux for 5 min under nitrogen atmosphere, and then a solution of compound **S2** (1.92 g, 10.88 mmol) in dry CH_3CN (15 mL) was added. The solution was heated at reflux for 22 hours. After the solid was filtered, the solvent was removed by evaporation on a rotary evaporator. The residue was purified by column chromatography on silica gel to give compound **5** as a white solid (564 mg, 69%). ^{1}H NMR (400 MHz, $CDCl_3$): δ 6.81 (s, 4H), 3.94-3.90 (t, J = 8.0 Hz, 4H), 2.40-2.37 (t, J = 6.0 Hz, 4H), 1.83-1.71 (m, 8H), 1.67-1.62 (m, 4H). ^{13}C NMR (126 MHz, $CDCl_3$):

δ 153.19, 119.75, 115.51, 68.06, 28.68, 25.54, 25.32, 17.26. MS (MALDI-TOF): Calculated for $[\mathbf{5}]^+$: 300.4; Found: 300.3.

Section C. Host-guest complexation studies in dilute solution.

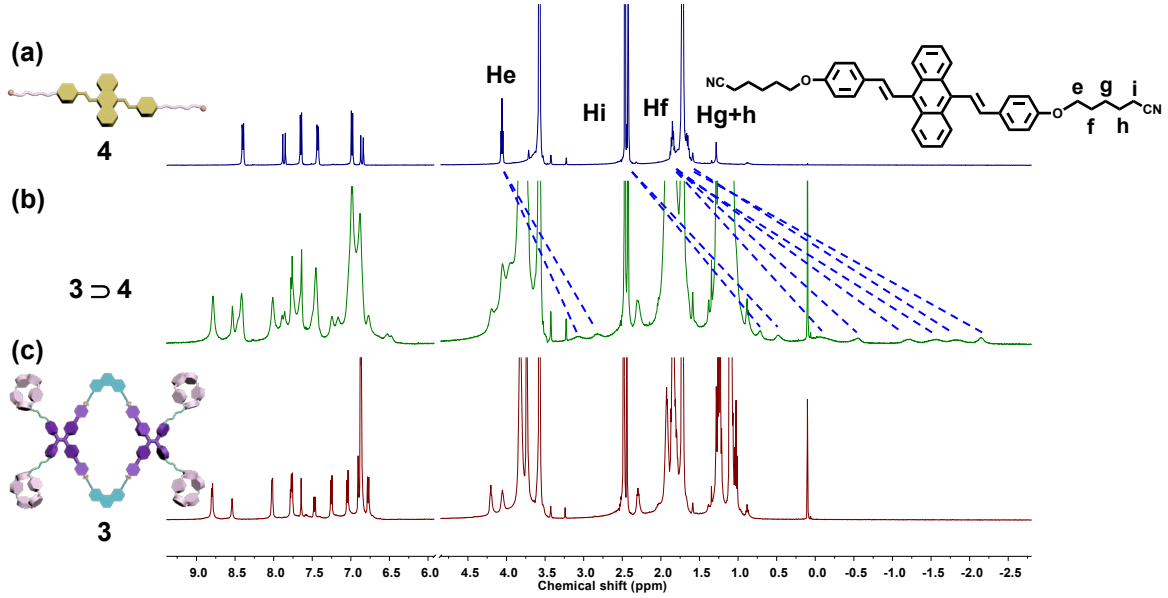

Fig. S4. The partial ^{1}H NMR spectra (500 MHz, THF-d_8, 298 K) of 2.0 mM dinitrile guest **4** (**a**), 2.0 mM **4** + 1.0 mM **3** (**b**) and metallacycle **3** (**c**).

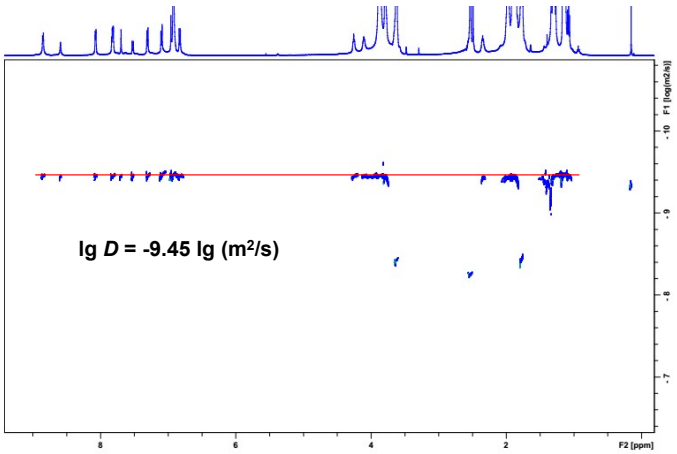

Fig. S5. 2D DOSY NMR (500 MHz, THF-d_8, 298 K) spectrum of metallacycle **3**.

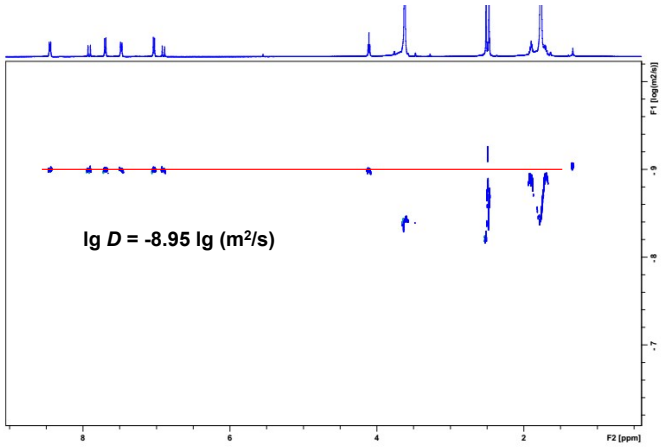

Fig. S6. 2D DOSY NMR (500 MHz, THF-d_8, 298 K) spectrum of dinitrile guest **4**.

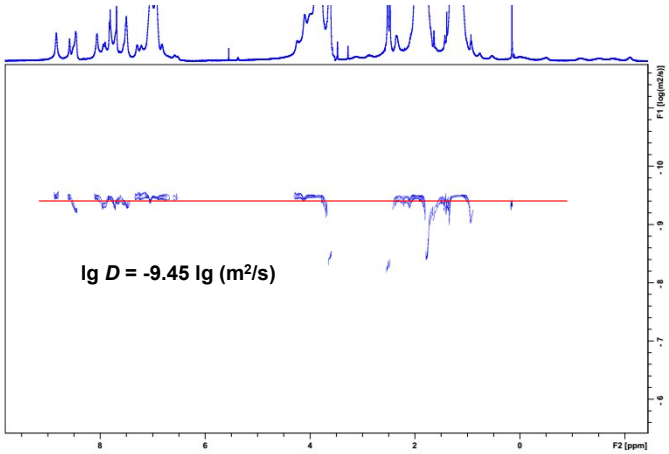

Fig. S7. 2D DOSY NMR (500 MHz, THF-d_8, 298 K) spectrum of host-guest complex **3** ⊃ **4**.

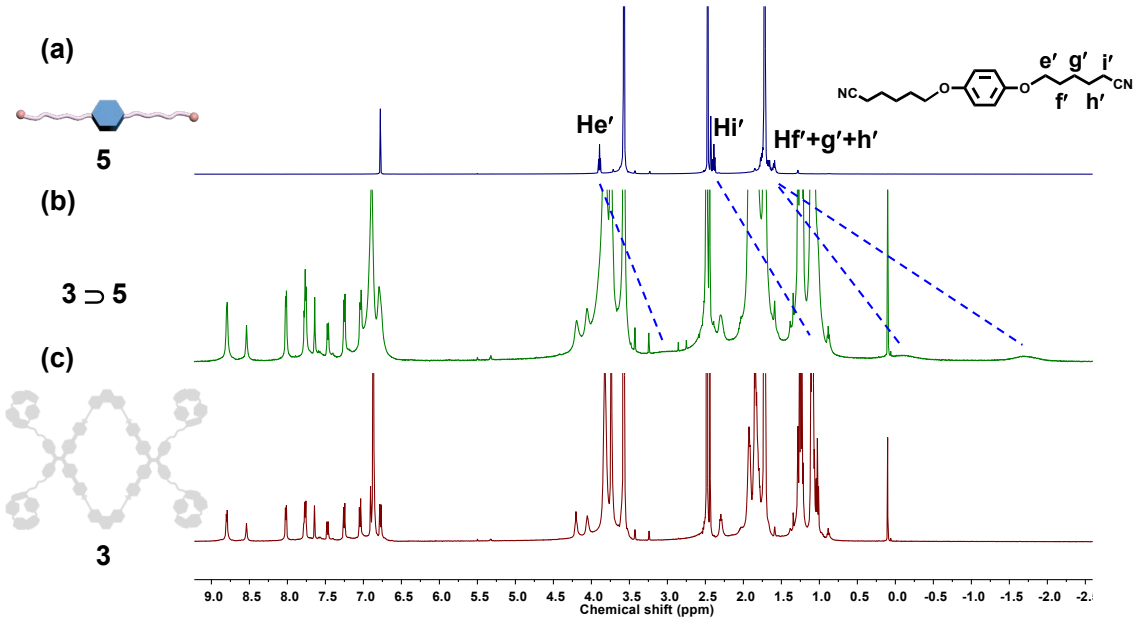

Fig. S8. The partial ^{1}H NMR spectra (500 MHz, THF-*d*, 298 K) of 2.0 mM dinitrile model guest **5** (**a**), 2.0 mM **5** + 1.0 mM **3** (**b**) and metallacycle **3** (**c**).

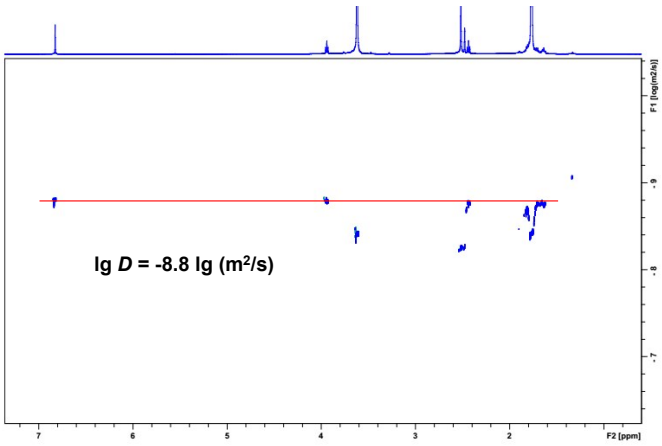

Fig. S9. 2D DOSY NMR (500 MHz, THF-d_8, 298 K) spectrum of dinitrile model guest **5**.

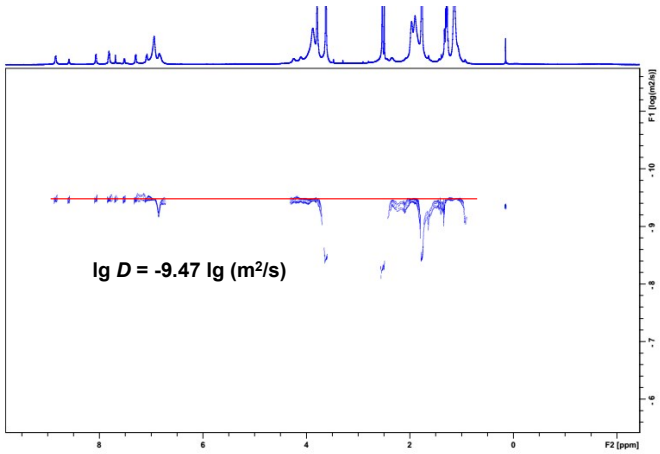

Fig. S10. 2D DOSY NMR (500 MHz, THF-d_8, 298 K) spectrum of host-guest complex **3** ⊃ **5**.

Section D. Photophysical properties study

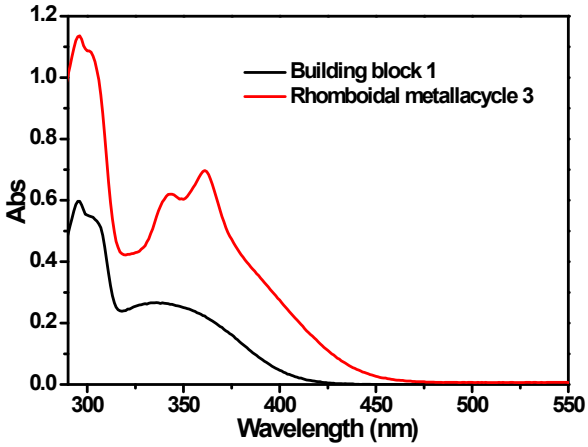

Fig. S11. Absorption spectra of building block **1** and rhomboidal metallacycle **3** in THF. ([TPE unit] = 10 μM).

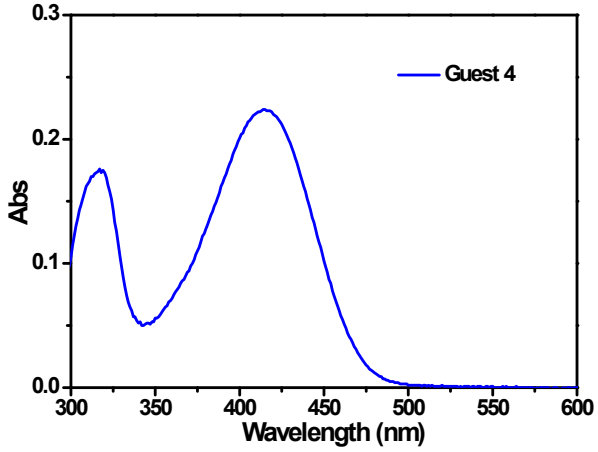

Fig. S12. Absorption spectra of guest **4** in THF. ([DSA unit] = 10 μM).

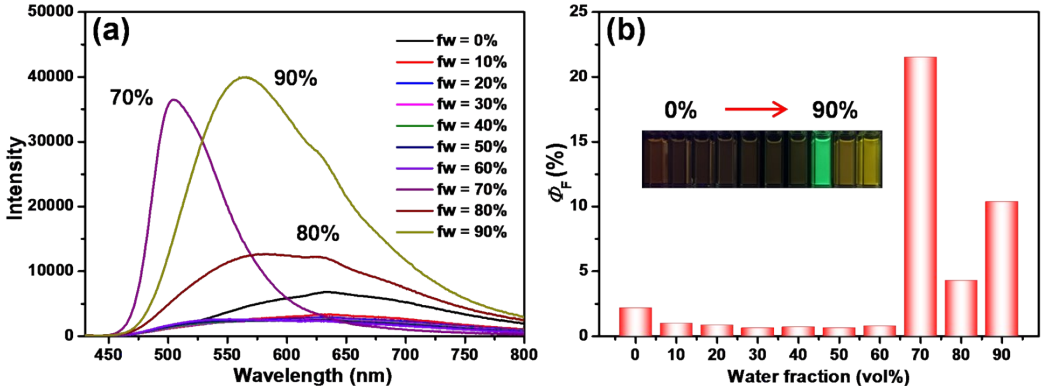

Fig. S13 Fluorescence emission spectra (a) and fluorescence quantum yield (b) of guest **4** versus the water fraction in the THF/water mixtures (λ_{ex} = 415 nm; slit widths: ex = 5 nm; em = 5 nm; [DSA unit] = 10 μM). Inset: Photographs of guest **4** (b) in THF/water mixtures with different fractions of water on excitation at 365 nm using an ultraviolet lamp at 298 K ([DSA unit] = 10 μM).

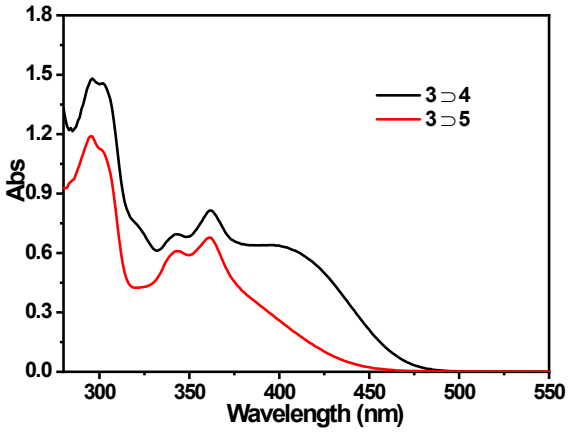

Fig. S14 Absorption spectra of **3** ⊃ **4** and **3** ⊃ **5** in THF. ([TPE unit] = 10 μM, [DSA unit] = 20 μM,).

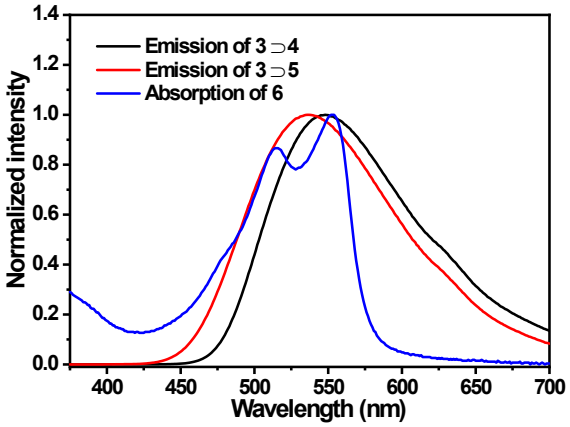

Fig. S15 Normalized emission spectrum of **3** ⊃ **4** (black line) and **3** ⊃ **5** (red line), and the absorption spectrum of acceptor **6** (blue line) in the mixture solution of THF/water (1:9, v/v). ([TPE unit] = 10 μM, [DSA unit] = 20 μM, [DPP unit] = 10 μM).

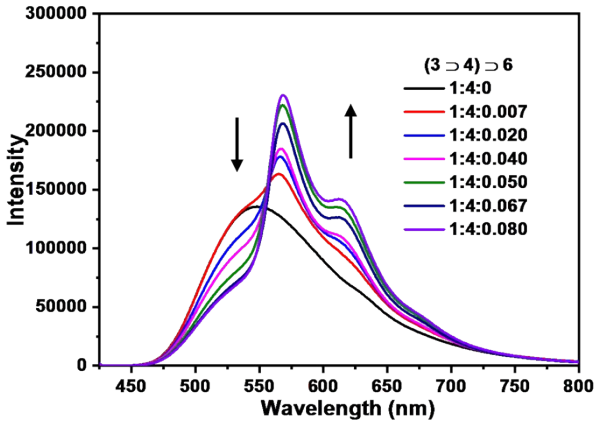

Fig. S16 Fluorescence emission spectra of (**3** ⊃ **4**) ⊃ **6** with different concentration of acceptor **6** in the mixtures of THF/water (1:9, v/v). (λ_{ex} = 415 nm, slit widths: ex = 5 nm, em = 5 nm, [TPE unit] = 10 μM, [DSA unit] = 20 μM, [DPP] = 0, 0.03, 0.10, 0.20, 0.25, 0.33, 0.40 μM).

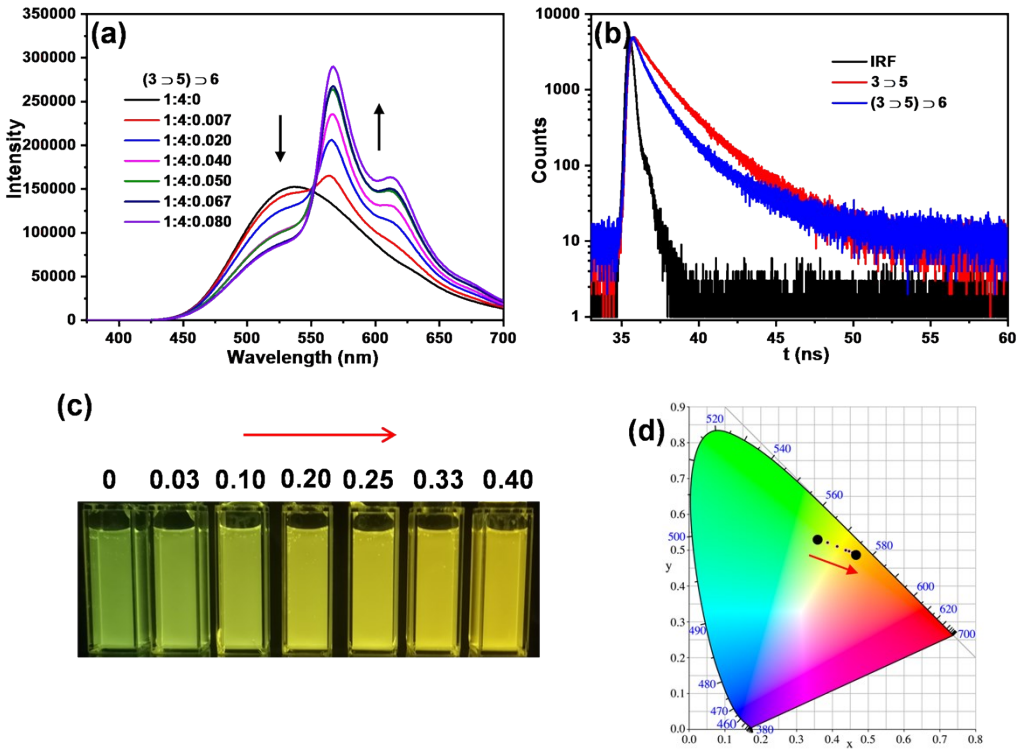

Fig. S17 Fluorescence emission spectra of (**3** ⊃ **5**) ⊃ **6** with different concentration of acceptor **6** (a), fluorescence decay profiles of **3** ⊃ **5** (red line) and (**3** ⊃ **5**) ⊃ **6** (blue line) (b), Photographs of (**3** ⊃ **5**) ⊃ **6** with different concentration of acceptor **6** on excitation at 365 nm using an ultraviolet lamp at 298 K (c), fluorescence emission of (**3** ⊃ **5**) ⊃ **6** in the CIE coordinates with different concentrations of acceptor **6** (d) in the mixtures of THF/water (1:9, v/v). (λ_{ex} = 361 nm, slit widths: ex = 5 nm, em = 5 nm, [TPE unit] = 10 μM, [DSA unit] = 20 μM, [DPP unit] = 0, 0.03, 0.10, 0.20, 0.25, 0.33, 0.40 μM).

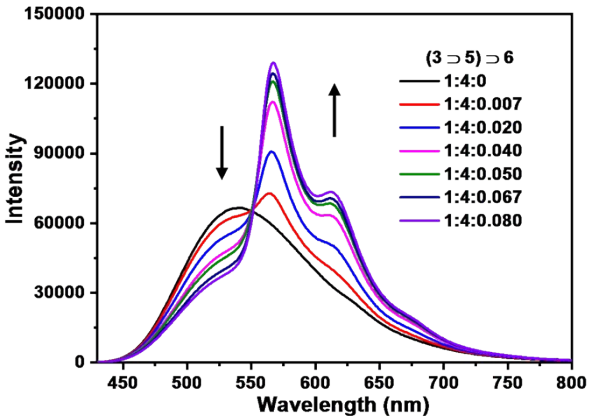

Fig. S18 Fluorescence emission spectra of (**3** ⊃ **5**) ⊃ **6** with different concentration of acceptor **6** in the mixtures of THF/water (1:9, v/v). (λ_{ex} = 415 nm, slit widths: ex = 5 nm, em = 5 nm, [TPE unit] = 10 μM, [DSA unit] = 20 μM, [DPP unit] = 0, 0.03, 0.10, 0.20, 0.25, 0.33, 0.40 μM).

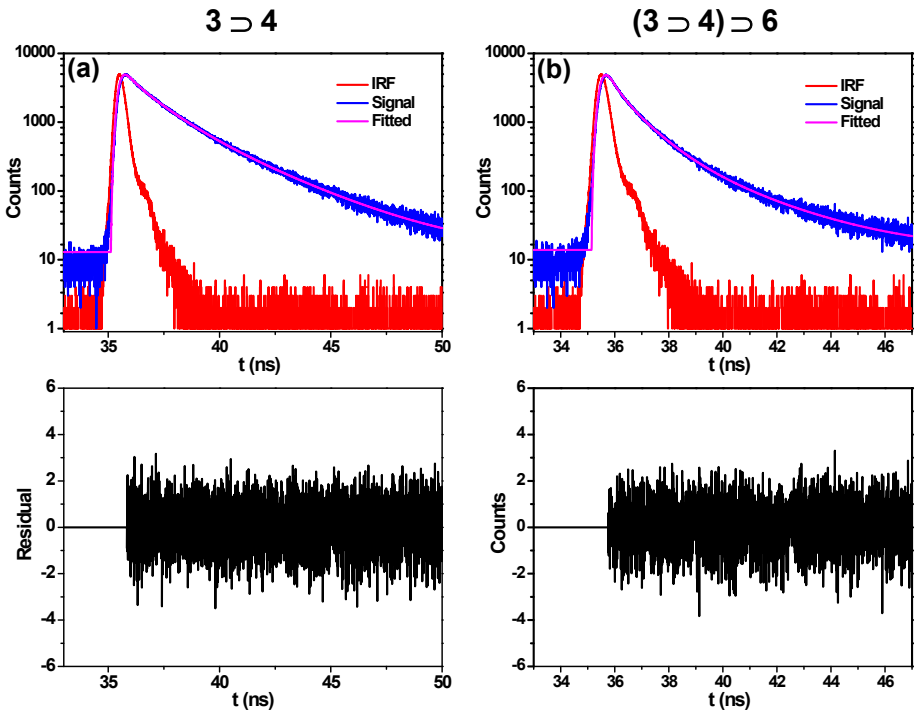

Fig. S19 Time-resolved fluorescence decay curves of **3** ⊃ **4** (a) and (**3** ⊃ **4**) ⊃ **6** (b), at 340 nm in the mixtures of THF/water (1:9, v/v) in air. Fitted by convoluting the IRF from the scattering of SiO_2 nanoparticles. ([TPE unit] = 10 μM, [DSA unit] = 20 μM, [DPP unit] = 0.40 μM).

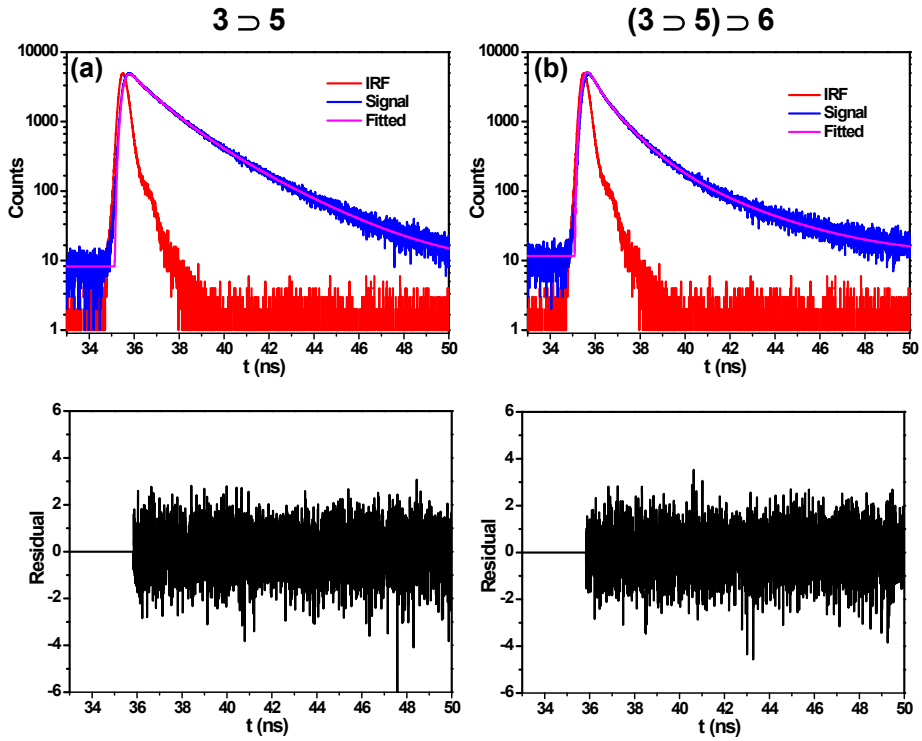

Fig. S20 Time-resolved fluorescence decay curves of **3** ⊃ **5** (a) and (**3** ⊃ **5**) ⊃ **6** (b), at 340 nm in the mixtures of THF/water (1:9, v/v) in air. Fitted by convoluting the IRF from the scattering of SiO_2 nanoparticles. ([TPE unit] = 10 μM, [DSA unit] = 20 μM, [DPP unit] = 0.40 μM).

Table S1. The fluorescence lifetimes in the mixtures of THF/water (1:9, v/v) in air

		1	2	3	chisqr
3 ⊃ 4	**Lifetime/ns**	1.3	0.42	3.1	1.01
	Percent/%	56	18	26	
	Average/ns	2.2			
		1	**2**	**3**	**chisqr**
(3 ⊃ 4) ⊃ 6	**Lifetime/ns**	0.95	2.7	0.34	1.01
	Percent/%	51	9	40	
	Average/ns	1.33			

Table S2. The fluorescence lifetimes in the mixtures of THF/water (1:9, v/v) in air

		1	2	3	chisqr
3 ⊃ 5	**Lifetime/ns**	2.6	1.2	0.25	1.04
	Percent/%	25	58	17	
	Average/ns	1.82			
		1	**2**	**3**	**chisqr**
(3 ⊃ 5) ⊃ 6	**Lifetime/ns**	3.0	1.0	0.36	1.04
	Percent/%	7	53	40	
	Average/ns	1.42			

Section E. Calculations of energy transfer efficiency (Φ_{ET}) and antenna effect

1. Energy transfer efficiency (Φ_{ET})

$$\Phi_{ET} = 1 - \frac{I_{DA}}{I_D}$$

Energy transfer efficiency, Φ_{ET}, the fraction of the absorbed energy that is transferred to the acceptor is experimentally measured as a ratio of the fluorescence intensities of the donor in the absence and presence of the acceptor (I_D and I_{DA}).

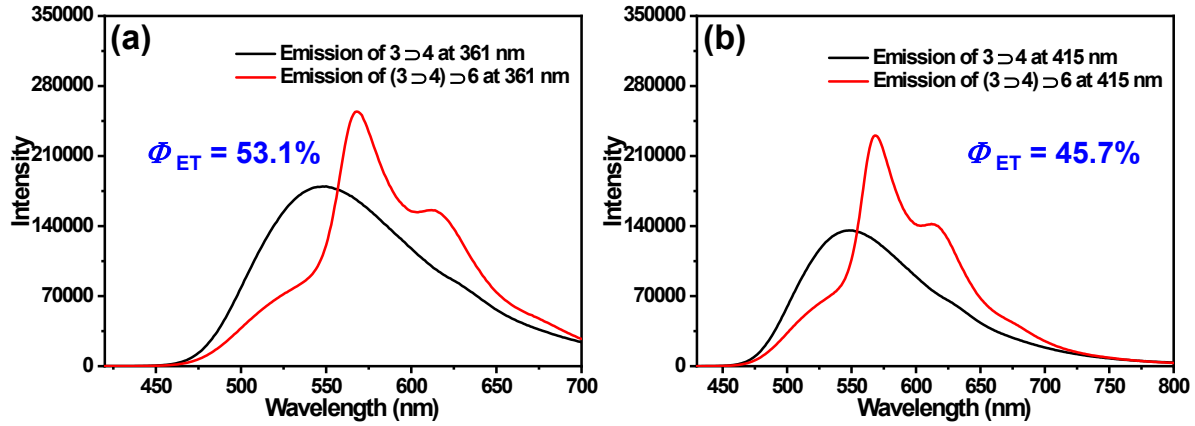

Fig. S21 Fluorescence emission spectra of **3** ⊃ **4** (black line) and (**3** ⊃ **4**) ⊃ **6** (red line) (λ_{ex} = 361 nm) (a) and (λ_{ex} = 415 nm) (b) in the mixtures of THF/water (1:9, v/v). (slit widths: ex = 5 nm, em = 5 nm, [TPE unit] = 10 μM, [DSA unit] = 20 μM, [DPP unit] = 0.40 μM).

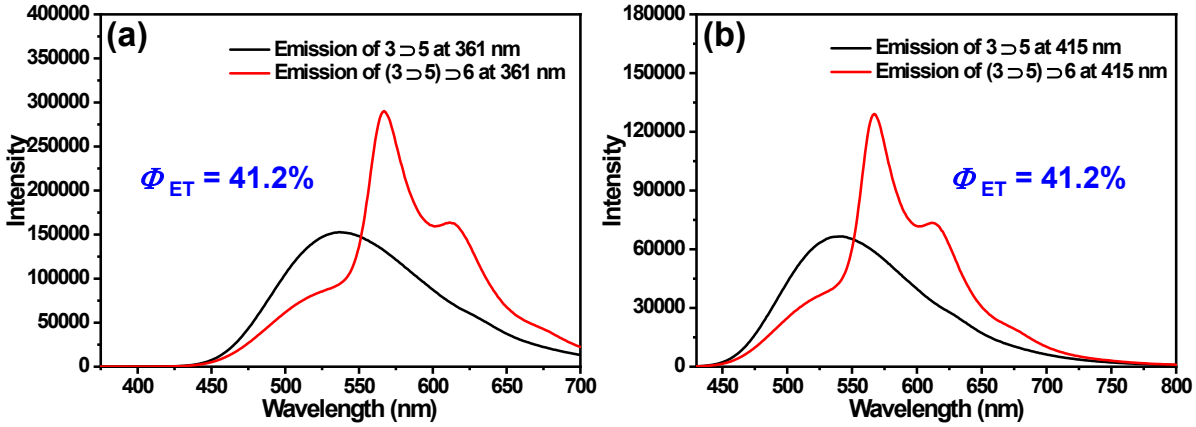

Fig. S22 Fluorescence emission spectra of **3** ⊃ **5** (black line) and (**3** ⊃ **5**) ⊃ **6** (red line) (λ_{ex} = 361 nm) (a) and (λ_{ex} = 415 nm) (b) in the mixtures of THF/water (1:9, v/v). (slit widths: ex = 5 nm, em = 5 nm, [TPE unit] = 10 μM, [Phenyl unit] = 20 μM, [DPP unit] = 0.40 μM).

2. Antenna effect

The antenna effect under certain concentrations of donor and acceptor equals the ratio of the emission intensity at 568 nm of the acceptor upon excitation of the donor.

$$\textbf{Antenna effect} = \frac{I^{568\ nm}_{A+D\ (\lambda_{ex}\,=\,361\ nm)} - I^{568\ nm}_{D\ (\lambda_{ex}\,=\,361\ nm)}}{I^{568\ nm}_{A+D\ (\lambda_{ex}\,=\,550\ nm)}}$$

where I_{A+D} (λ_{ex} = 361 nm or 415 nm) and I_{A+D} (λ_{ex} = 550 nm) are the fluorescence intensities of excitation of the donor at 361 nm or 415 nm and direct excitation of the acceptor at 550 nm, respectively.

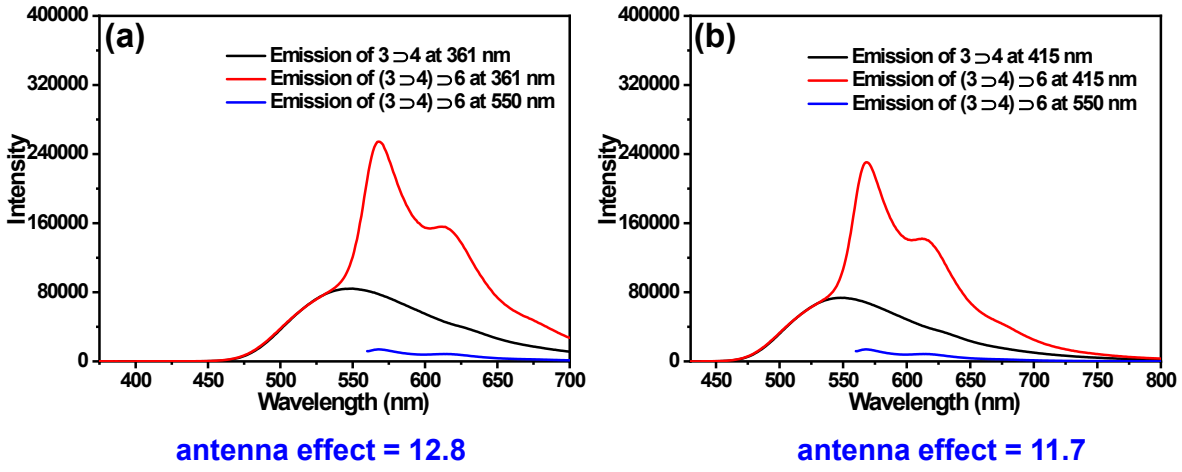

Fig. S23 Fluorescence emission spectra of (**3** ⊃ **4**) ⊃ **6**, red line (λ_{ex} = 361 nm) and blue line (λ_{ex} = 550 nm), **3** ⊃ **4**, black line (λ_{ex} = 361 nm, normalized according to the fluorescence intensity at 530 nm of the red line) (a), fluorescence emission spectra of (**3** ⊃ **4**) ⊃ **6**, red line (λ_{ex} = 415 nm) and blue line (λ_{ex} = 550 nm), **3** ⊃ **4**, black line (λ_{ex} = 415 nm, normalized according to the fluorescence intensity at 530 nm of the black line) (b) in the mixtures of THF/water (1:9, v/v). (slit widths: ex = 5 nm, em = 5 nm, [TPE unit] = 10 μM, [DSA unit] = 20 μM, [DPP unit] = 0.40 μM).

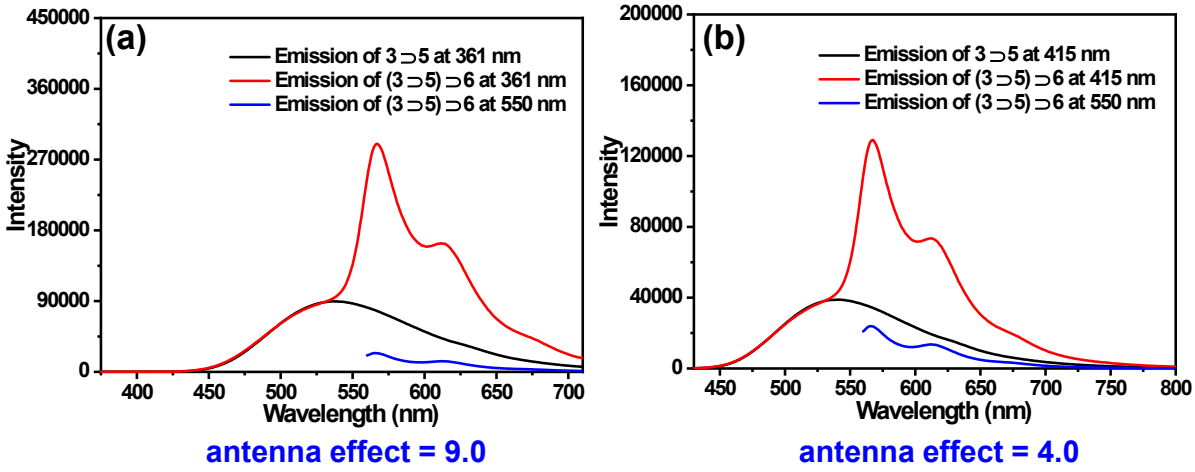

Fig. S24 Fluorescence emission spectra of (**3** ⊃ **5**) ⊃ **6**, red line (λ_{ex} = 361 nm) and blue line (λ_{ex} = 550 nm), **3** ⊃ **5**, black line (λ_{ex} = 361 nm, normalized according to the fluorescence intensity at 530 nm of the red line) (a), fluorescence emission spectra of (**3** ⊃ **5**) ⊃ **6**, red line (λ_{ex} = 415 nm) and blue line (λ_{ex} = 550 nm), **3** ⊃ **5**, black line (λ_{ex} = 415 nm, normalized according to the fluorescence intensity at 530 nm of the black line) (b) in the mixtures of THF/water (1:9, v/v). (slit widths: ex = 5 nm, em = 5 nm, [TPE unit] = 10 μM, [Phenyl unit] = 20 μM, [DPP unit] = 0.40 μM).

Section F. Supplementary data

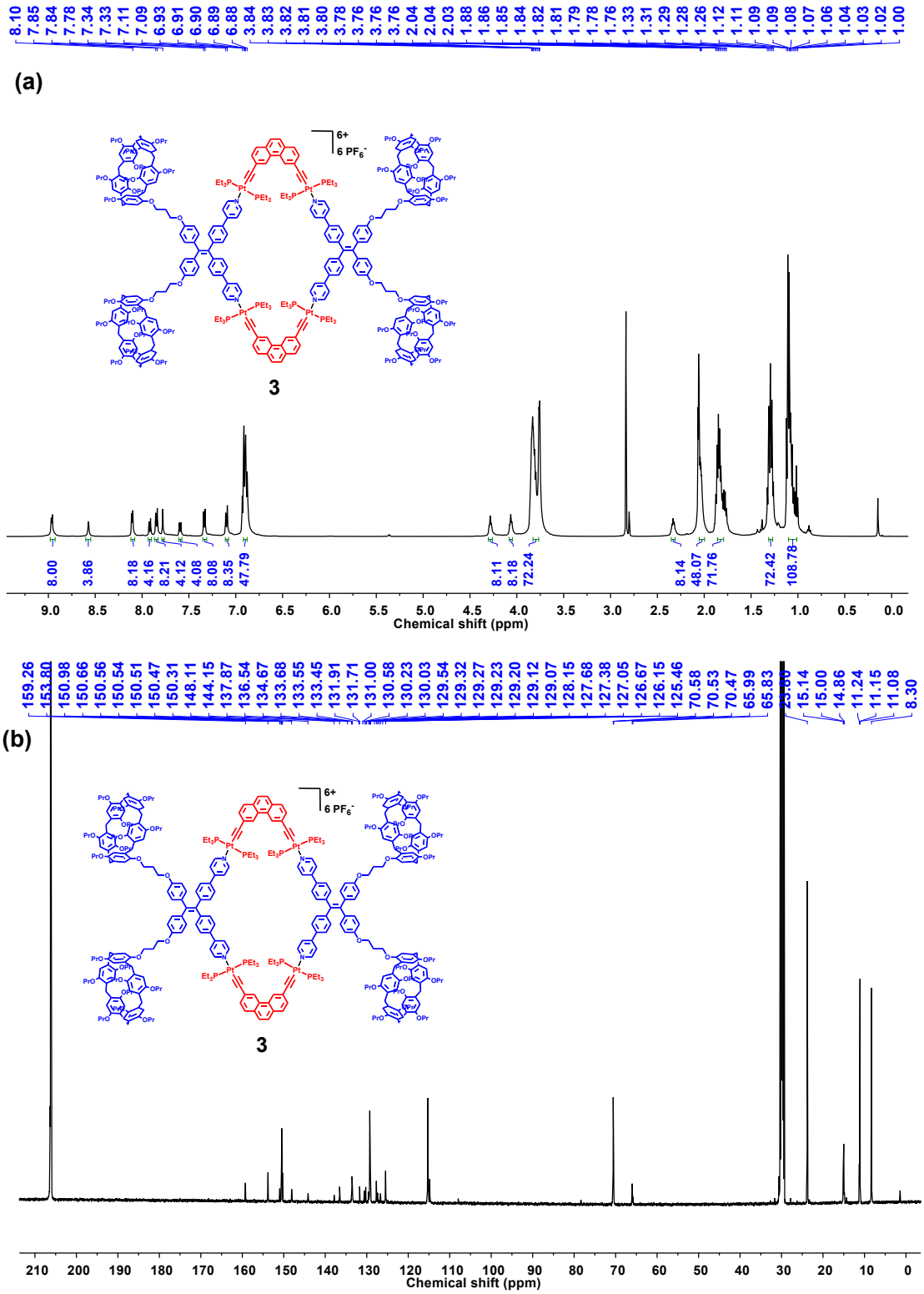

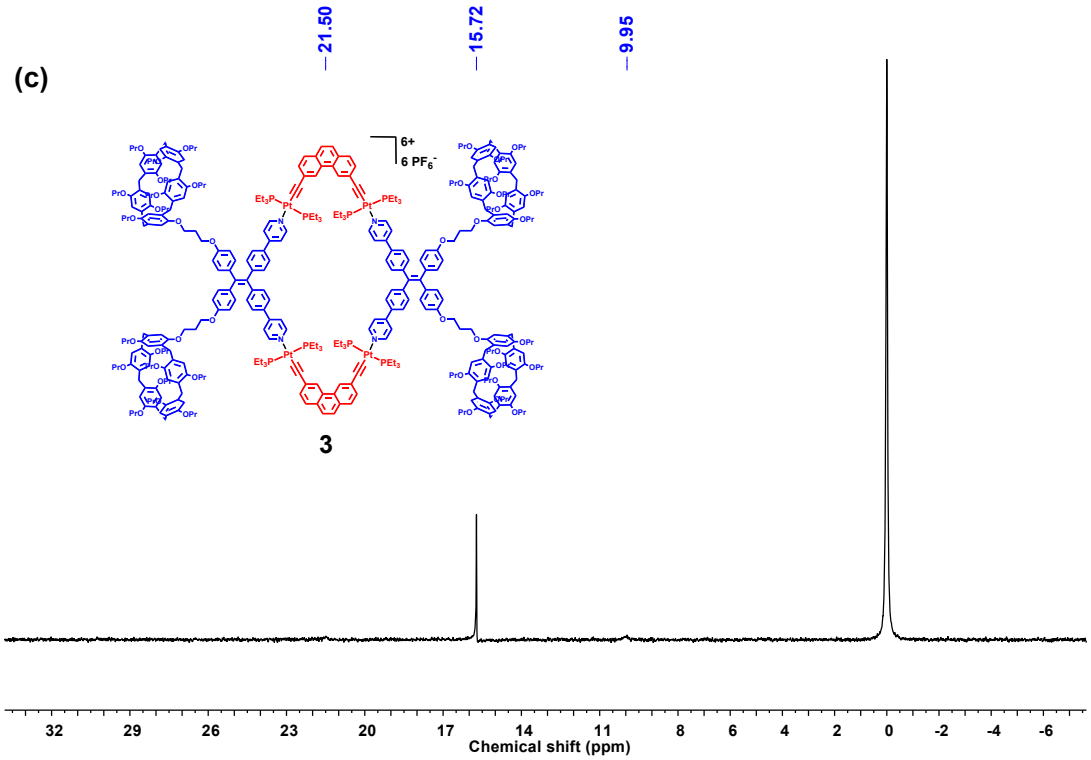

Fig. S25. (a) ^{1}H NMR spectrum (500 MHz, acetone-d_6, 298 K), (b) ^{13}C NMR spectrum (126 MHz, acetone-d_6, 298 K), (c) ^{31}P NMR spectrum (202 MHz, acetone-d_6, 298 K) of metallacycle **3**.

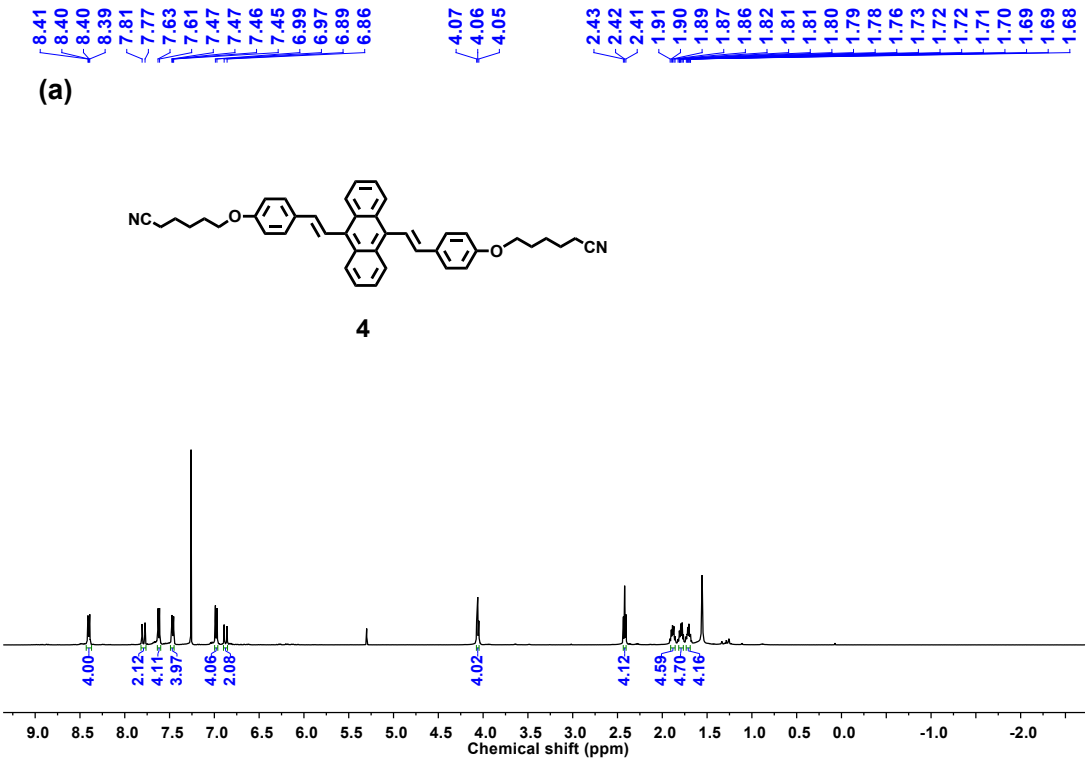

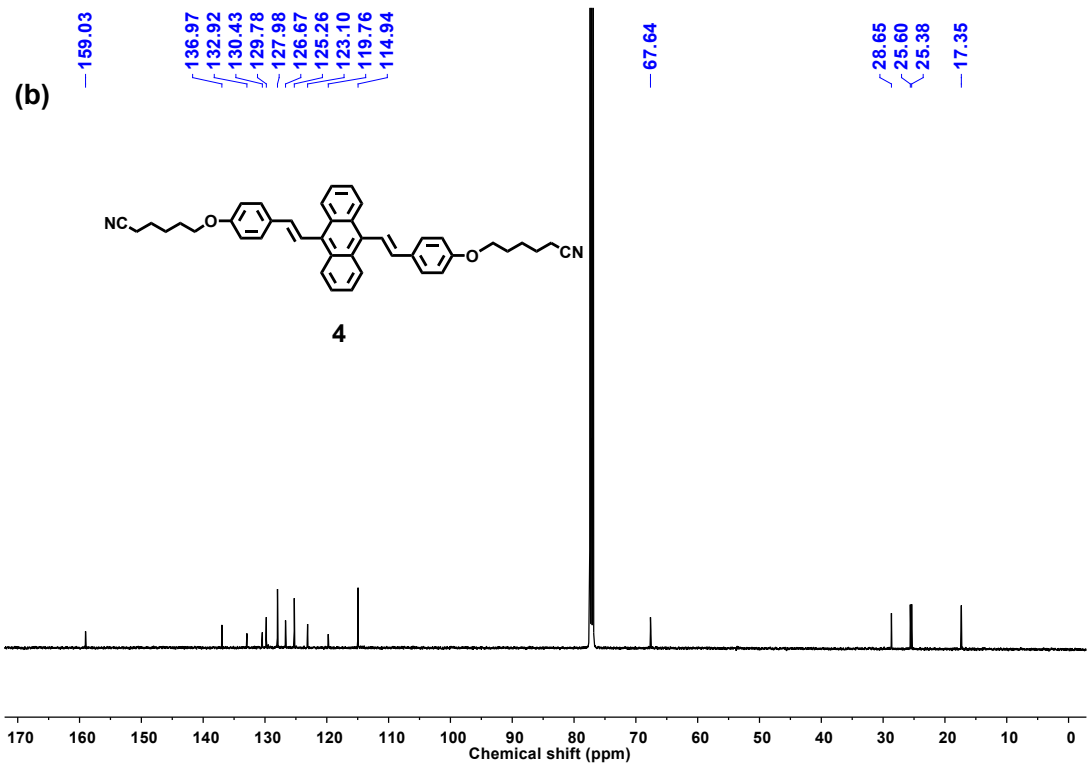

Fig. S26. (a) ^{1}H NMR spectrum (500 MHz, $CDCl_3$, 298 K), (b) ^{13}C NMR spectrum (126 MHz, $CDCl_3$, 298 K) of compound **4**.

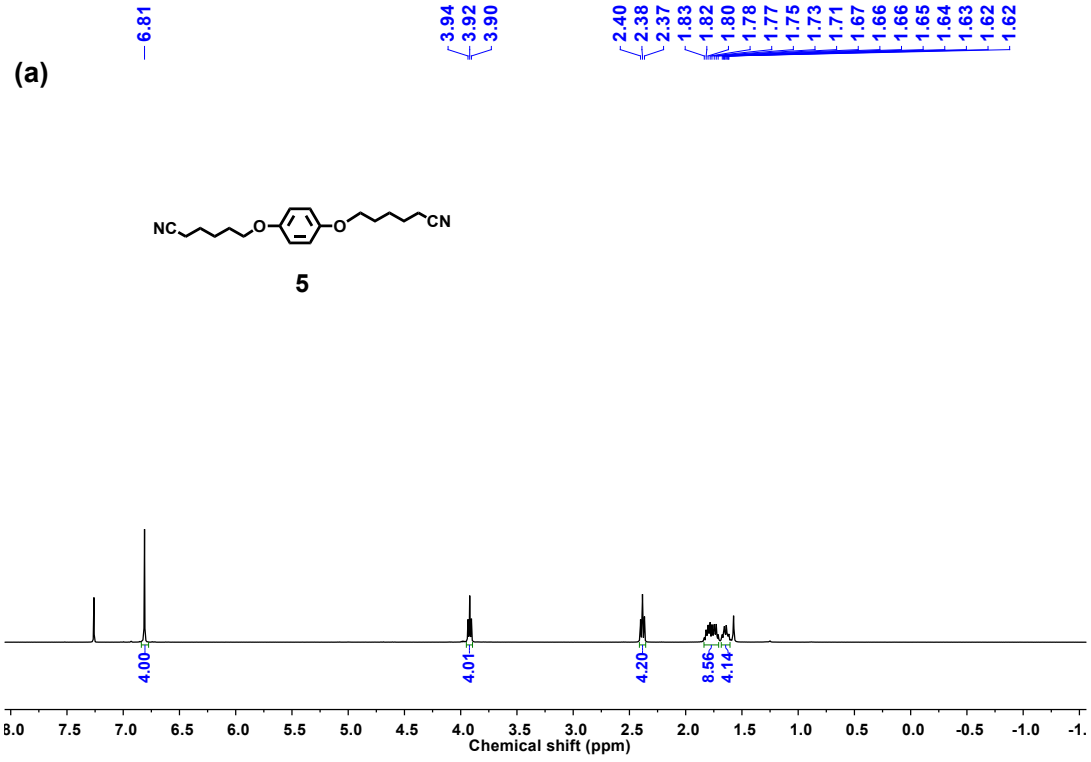

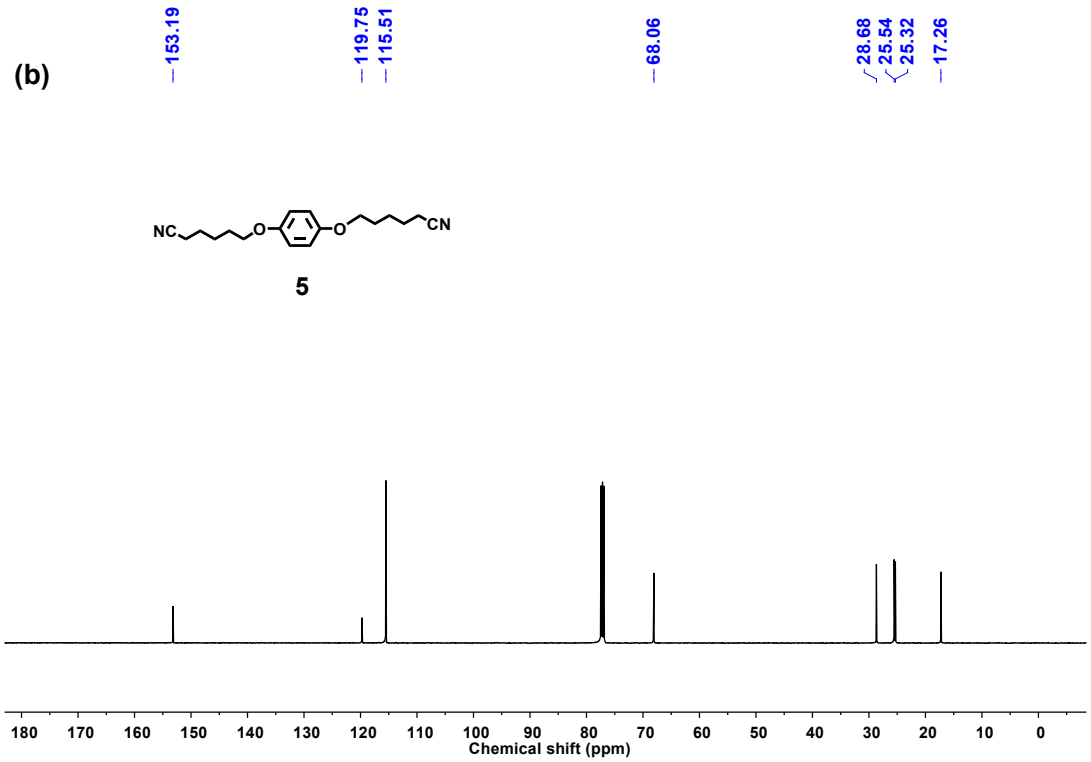

Fig. S27. (a) ^{1}H NMR spectrum (400 MHz, $CDCl_3$, 298 K), (b) ^{13}C NMR spectrum (126 MHz, $CDCl_3$, 298 K) of compound **5**.

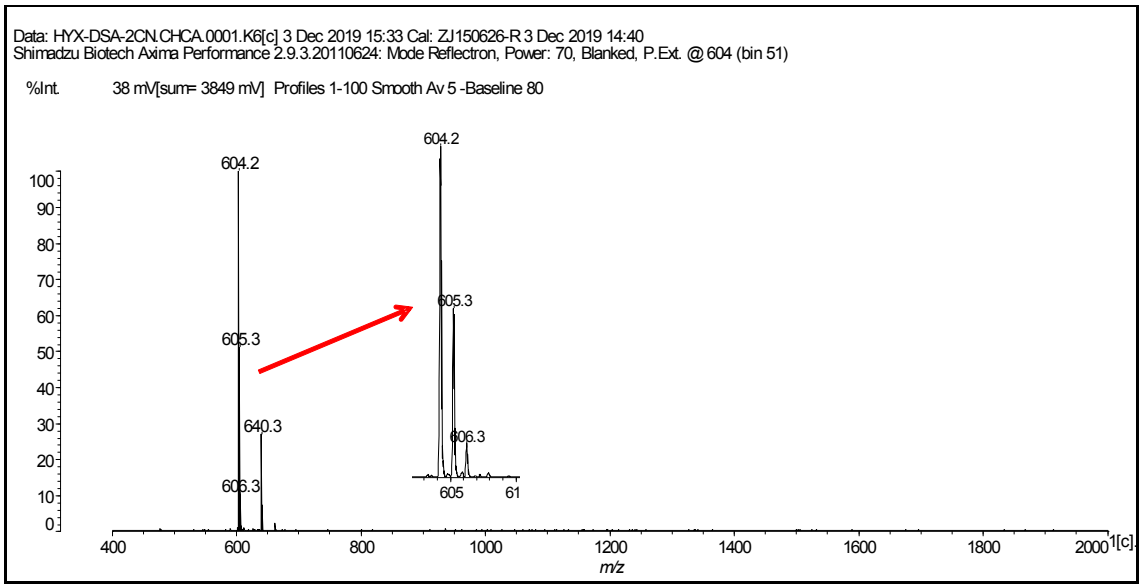

Fig. S28. MALDI-TOF-MS for compound **4**: calcd for $[\mathbf{4}]^{+}$: 604.3, found: 604.2.

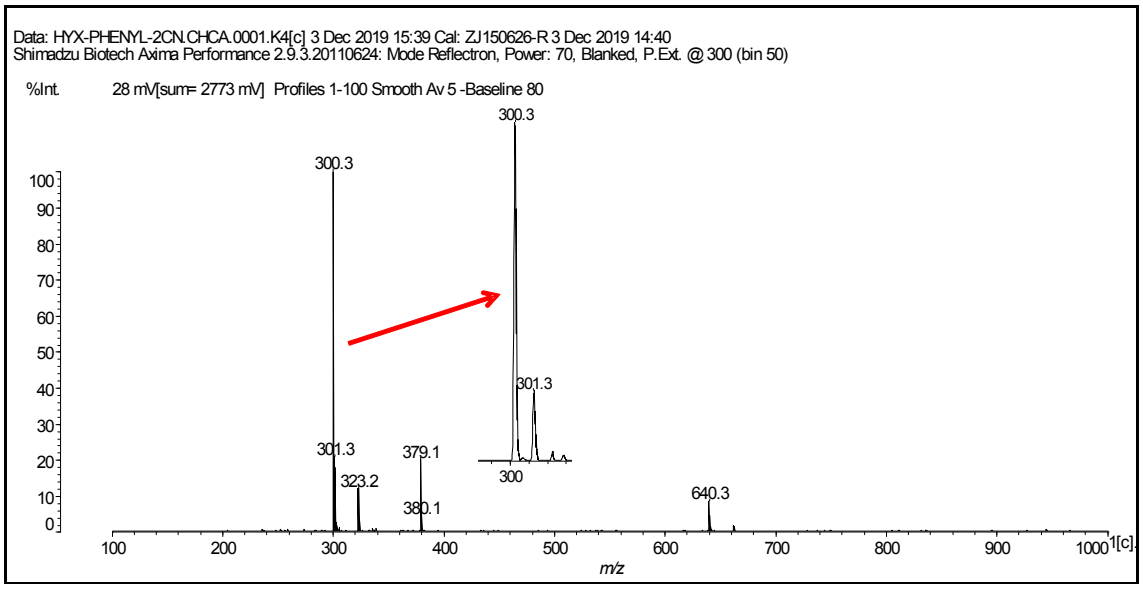

Fig. S29. MALDI-TOF-MS for compound **5**: calcd for $[\mathbf{5}]^{+}$: 300.4, found: 300.3.

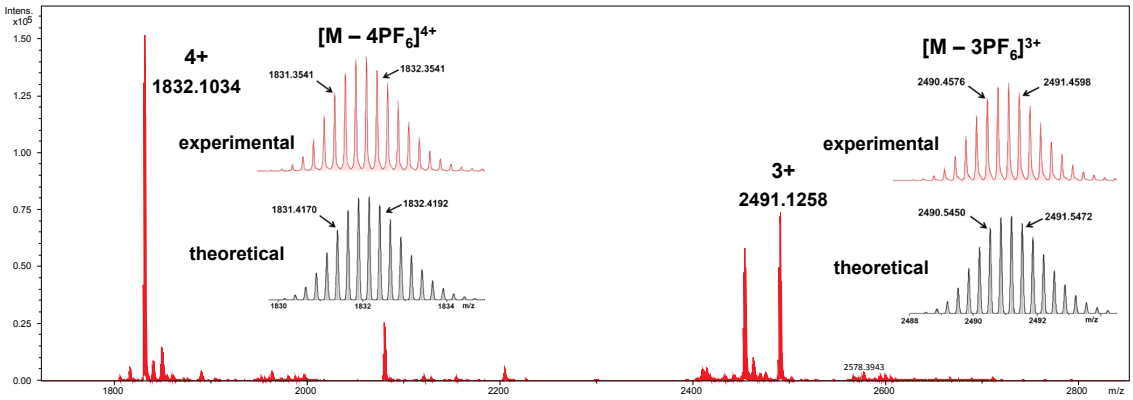

Fig. S30. Full ESI-TOF-MS spectra of metallacycle **3**. Inset: Theoretical and experimental ESI-TOF-MS spectra of metallacycle **3**.

Section G. References

S1. C.-W. Zhang, B. Ou, S.-T. Jiang, G.-Q. Yin, L.-J. Chen, L. Xu, X. Li and H.-B. Yang, *Polym. Chem.,* 2018, **9**, 2021.

S2. H.-B. Yang, K. Ghosh, A. M. Arif and P. J. Stang, *J. Org. Chem.,* 2006, **71**, 9464.

S3. C.-L. Sun, H.-Q. Peng, L.-Y. Niu, Y.-Z. Chen, L.-Z. Wu, C.-H. Tung and Q.-Z. Yang, *Chem. Commun.,* 2018, **54**, 1117.